
MedDreamer: Model-Based Reinforcement Learning with Latent Imagination on Complex EHRs for Clinical Decision Support

Qianyi Xu

National University of Singapore
e0673214@u.nus.edu

Gousia Habib

National University of Singapore
gousiya1@nus.edu.sg

Dilruk Perera *

National University of Singapore
dilruk@nus.edu.sg

Mengling Feng

National University of Singapore
ephfm@nus.edu.sg

Abstract

Timely and personalized treatment decisions are essential across a wide range of healthcare settings where patient responses vary significantly and evolve over time. Clinical data used to support these decisions are often irregularly sampled, sparse, and noisy. Existing decision support systems commonly rely on discretization and imputation, which can distort critical temporal dynamics and degrade decision quality. Moreover, they often overlook the clinical significance of irregular recording frequencies, filtering out patterns in how and when data is collected. Reinforcement Learning (RL) is a natural fit for clinical decision-making, enabling sequential, long-term optimization in dynamic, uncertain environments. However, most existing treatment recommendation systems are model-free and trained solely on offline data, making them sample-inefficient, sensitive to data quality, and poorly generalizable across tasks or cohorts. To address these limitations, we propose MedDreamer, a two-phase model-based RL framework for personalized treatment recommendation. MedDreamer uses a world model with an Adaptive Feature Integration (AFI) module to effectively model irregular, sparse clinical data. Through latent imagination, it simulates plausible patient trajectories to enhance learning, refining its policy using a mix of real and imagined experiences. This enables learning policies that go beyond suboptimal historical decisions while remaining grounded in clinical data. To our knowledge, this is the first application of latent imagination to irregular healthcare data. Evaluations on sepsis and mechanical ventilation (MV) treatment using two large-scale EHR datasets show that MedDreamer outperforms both model-free and model-based baselines in clinical outcomes and off-policy metrics.

1 Introduction

Unlike traditional one-size-fits-all approaches, modern healthcare systems increasingly prioritize personalized treatment recommendations that account for inter- and intra-patient variations. This is especially important in clinical care settings such as intensive care units (ICUs), where prompt individualized interventions can considerably improve patient outcomes. RL is considered a natural fit for this task, as it enables agents to navigate complex conditions independently and potentially identify effective strategies without relying on predefined, optimal policies. Unlike traditional RL

*Correspondence to dilruk@nus.edu.sg

methods applied in game playing or robotics [8, 43], real-world exploration during training is not feasible in healthcare, due to ethical constraints. Learning complex treatment policies is challenging in this offline setting, as healthcare data is limited and often lacks sufficient variability needed to generalize across diverse patient populations and clinical scenarios [29, 27].

To address these challenges, we adopt a model-based RL approach, which enables sampling patient trajectories from a world model, allowing extensive exploration within ethical boundaries. Despite its promise, model-based RL remains underexplored in healthcare due to the unique challenges posed by clinical data. The nature of EHRs, characterized by their irregular sampling, missing values, sparsity, and significant variability, make it challenging to build a world model that accurately captures the complex dynamics of patients and their interactions with treatments[2]. Furthermore, it is essential to ground the learned policy on real-world data to ensure clinical relevance. The learned policy must closely align with successful clinical practices, deviating only when necessary to accommodate new insights or unobserved scenarios, while maintaining generalizability across varied patient conditions.

Accordingly, we propose MedDreamer, a novel patient latent dynamics model that addresses the unique challenges of healthcare treatment optimization by capturing patient-specific dynamics in a compact, structured latent space. MedDreamer extends the recent advances in latent dynamics modeling [13, 5, 36] to the healthcare domain, where small but sudden changes in patient condition can be clinically significant. Furthermore, we distance our world model from standard deterministic approaches [9, 4, 38, 3] used in the literature that operate directly in observation space, which is high-dimensional, highly varying and sparse in our case. In contrast, MedDreamer captures temporal dynamics in a denoised, dense and more structured latent space tailored for treatment policy optimization.

MedDreamer introduces a novel AFI module to address inherent data challenges in EHRs, including sparsity, irregular sampling, and loss of temporal context. Existing solutions often introduce bias and distortions into the state space by discretizing patient trajectories into fixed time windows (e.g., 4 hourly) and imputing missing values using heuristics such as the mean or median[18]. Although such methods were necessary for model training in prior literature, they distort the temporal underlying temporal trends and clinical progression, misrepresenting the real-world clinical realities. The proposed AFI module operates directly on original features and incorporates elapsed time and missingness indicators, enabling accurate modeling of irregular and sparse data without error-prone imputations.

Furthermore, MedDreamer introduces a novel two-phased policy training strategy to address the limitations of offline and ethically constrained learning. In the first phase, the policy is heavily trained on retrospective patient trajectories followed by a few imagined steps at the end of trajectory, establishing a clinically grounded treatment policy. In the second phase, the learned policy is refined using full imagination from every state on the trajectory, allowing for exploration of counterfactual and unobserved scenarios. Unlike common practice that train solely on imagined data [13], MedDreamer explicitly mixes real and simulated trajectories, balancing generalization with clinical reliability.

We evaluate our solution on two clinical making tasks: sepsis treatment recommendation and mechanical ventilation management. Sepsis is a multi-organ disease involving a large, highly variable and complex feature space. Furthermore, there is no standardized sepsis treatment policy available and current practices are believed to cause harm to some patients [30, 23]. Similarly, ventilation strategies lack universally accepted protocols and require patient-specific decision making. These challenges call for an effective data-driven solution capable of generalizing beyond the limited and retrospective clinical data to learn better treatment policies. MedDreamer adheres to clinical ethics by relying solely on retrospective public datasets and serving strictly as a decision support tool (Detailed discussion in Appendix A: Ethical Statement).

Our main contributions are as follows: First, to the best of our knowledge, MedDreamer is the first formalized latent dynamics model to effectively learn patient dynamics for treatment recommendations. Second, the AFI module captures patient and treatment dynamics by modeling their interactions in higher-order latent spaces, effectively addressing the challenges of irregular sampling, sparsity, and missing values inherent in EHR data. Moreover, we propose a two-phased framework that grounds the policy in real clinical time progression and refines it using horizon-based imagination mixed with real data, enabling robust exploration without sacrificing clinical reliability. Finally, we comprehensively evaluate our framework on two large real-world datasets on the complex sepsis

treatment and mechanical ventilation management tasks, demonstrating better treatment efficacy and survival rates, with a relative mortality rate decrease of 20.86% and 16% compared to clinicians.

2 Related Work

Inspired by the success in domains such as robotics [40], game playing [28, 39] and autonomous driving [31], RL has been widely adopted for various healthcare treatment recommendation tasks[1] for both chronic [32, 44] and acute [15, 34] treatment recommendation tasks. However, the majority of these solutions rely on model-free RL, where treatment agents are trained using available limited retrospective EHR data. However, the inherent limitations in EHR data such as the limited quantity, and lack of coverage across diverse patient and clinical conditions, often lead to non-generalized treatment policies [47].

Model-based RL is a suitable approach to mitigate these issues, however, despite the potential, model-based RL remains underexplored [6, 25] as it is highly challenging to develop an accurate world model using noisy, highly variant, sparse and irregularly sampled data inherent in EHR data[14]. Available model-based treatment recommendation solutions operate on raw physiological measurement space where they are directly exposed to these data challenges[41]. In contrast, the proposed framework leverages latent patient dynamics to mitigate these issues, transforming raw features into a more structured and dense latent space. This approach enables the model to effectively learn treatment strategies, patient features, and their complex interconnections within this latent space.

Furthermore, unlike traditional model-based approaches that rely solely on world model-generated trajectories for policy learning[37, 21], we employ a two-phased approach to first ground the policy in real trajectories before introducing simulated rollouts. Similar to MedDreamer, prior offline MBRL methods such as COMBO[46] and MOPO[45] use both real and simulated data. However these sources are combined uniformly in training without explicit grounding and exploration phases, and operate directly in raw observation spaces, making it difficult to learn under noisy and irregular EHR data. Similarly, Dreamer-style models[10, 12, 13] use latent imagination but lack separation of grounding and exploration, and are not tailored to safety-critical domains. In contrast, MedDreamer introduces a structured two-phased policy learning approach for healthcare, mixing imagined and real data only during the refinement stage to ensure robust generalization and clinical reliability.

3 Methodology

Inspired by DreamerV3[13], MedDreamer introduces a tailored adaptation of latent imagination to the healthcare domain. However, due to unique challenges of clinical data, including irregularity, missingness, sparsity and high inter-patient variability it is difficult to directly train stable world models with policies end-to-end. Therefore, given the high variability in patient dynamics and the importance of capturing subtle physiological changes, we first train a reliable world model before proceeding to policy optimization. We also design a novel two-phase training scheme for policy to enable safe, ethically compliant, and clinically grounded exploration of counterfactual scenarios. The architecture is illustrated in Figure 1.

3.1 World Model for Irregular Data Handling

3.1.1 Adaptive Feature Integration (AFI) Module

We introduce a novel AFI Module to enhance the representation of clinical features by capturing intricate dependencies, while addressing the inherent data sparsity and irregularities in clinical data. The module consists of three main layers, namely Input Layer, Embedding Layer and a Higher Order Interaction Layer as follows.

Input Layer: The input Layer processes clinical observations (i.e., physiological measurements) and temporal information into a unified representation suitable for downstream feature transformations. These inputs are denoted as $x_t = \{o_t, \Delta_t\}$ where $o_t = \{o_{t,1}, o_{t,2}, \dots o_{t,p}\}$ represents p observed variables a $\Delta_t = \{\Delta_{t,1}, \Delta_{t,2}, \dots \Delta_{t,p}\}$ is the elapsed times since each feature was last recorded.

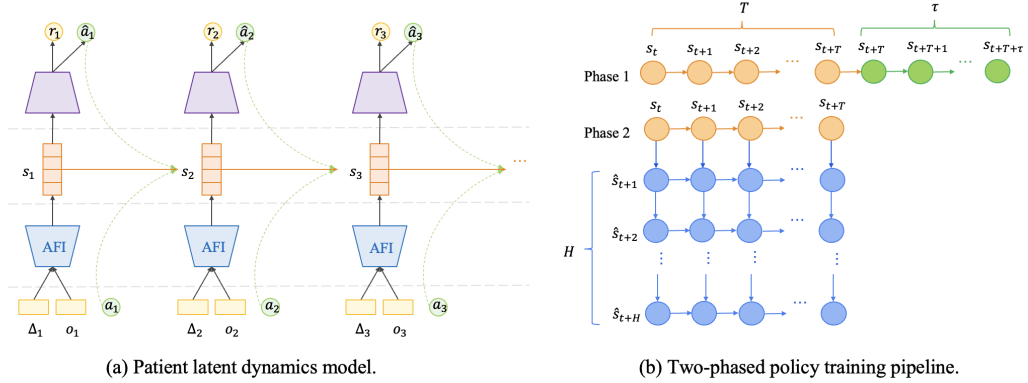


Figure 1: MedDreamer architecture. (a) The world model uses δ_t , o_t and clinician a_t to learn latent states through reconstruction and reward prediction. World model is then used to predict next states using policy actions \hat{a}_t . (b) Two-phased training for a single patient trajectory: Phase 1 imagines τ steps forward in time, and Phase 2 imagines H steps in the horizon space.

Accordingly, each j -th feature at time t can be described as $x_{t,j} = \{o_{t,j}, \Delta_{t,j}\}$ where the elapsed time $\Delta_{t,j}$:

$$\Delta_{t,j} = \begin{cases} o_t - o_{t-1} + \Delta_{t-1}^d & \text{if } t > 1, m_{t-1,j}^d = 0, \\ o_t - o_{t-1} & \text{if } t > 1, m_{t-1,j}^d = 1, \\ 0 & \text{if } t = 0. \end{cases} \quad (1)$$

Incorporating o_t and Δ_t in a unified representation establishes a robust framework to handle irregularities and sparsity inherent in clinical data. Simultaneously, the use of Δ_t per individual feature ensures that the temporal context of each feature is preserved, capturing the timing and impact of delayed and irregular observations on the patient’s trajectory. For example, consistent absence of a feature may denote a meaningful signal, indicating the feature may not be clinically relevant or routinely monitored for the individual. Such contextual information are often ignored in existing and widely practiced discretization and erroneous imputation techniques.

Embedding Layer: Each input feature $x_i \in x_t$ is transformed into a dense latent representation $e_i \in \mathbb{R}^k$, where k is the embedding dimensionality as $e_i = W_i x_i$, where $W_i \in \mathbb{R}^{k \times d_i}$ is a learnable feature transformation matrix. The embedding layer transforms sparse and highly variable continuous feature inputs into a compact and expressive latent space. This allows the model to capture more informative embeddings for each physiological feature and its corresponding time lapse, ensuring rich representations while offering resilience against missing data.

Higher Order Interaction Layer: To explicitly model the interactions between features, the higher-order interaction layer computes pairwise interactions between embeddings using element-wise products as $e_{ij} = e_i \odot e_j; i \neq j$. The output representation of the layer, denoted $x_t^{\text{HO}} = \{e_1, e_2, \dots, e_{ij}\}$, incorporates individual feature effects and pairwise interactions, modeling how individual feature effects and their time lapses influence each other, such as amplifying, complimenting or offsetting their impacts to provide a more informative representation of the patient states over time.

3.1.2 The Patient Dynamics Model

Consistent with prior works [13, 7], we learn patient dynamics using a Recurrent State-Space Model (RSSM) [11] which consists of a deterministic dynamics predictor and a categorical variational autoencoder (VAE) with 32 categories, each with 32 classes. While categorical latent variables are commonly used in image based inputs, we argue that they are also useful for modeling clinical time series data. Specifically, compared to Gaussian latent states used in DreamerV1 [10], categorical variables provide sharper, more discrete abstractions that better capture abrupt and clinically meaningful

state transitions. Model components and associated loss functions are summarized below.

$$\begin{aligned}
\text{Sequence model: } & h_t = f_\phi(h_{t-1}, z_{t-1}, a_{t-1}) \\
\text{AFI module: } & x_t^{\text{HO}} = f_\phi(o_t, \Delta_t) \\
\text{Encoder: } & z_t \sim q_\phi(z_t | h_t, x_t^{\text{HO}}) \\
\text{Dynamics predictor: } & \hat{z}_t \sim p_\phi(\hat{z}_t | h_t) \\
\text{Reward predictor: } & \hat{r}_t \sim p_\phi(\hat{r}_t | h_t, z_t) \\
\text{Continuation predictor: } & \hat{c}_t \sim p_\phi(\hat{c}_t | h_t, z_t) \\
\text{Decoder: } & \hat{x}_t \sim p_\phi(\hat{x}_t | h_t, z_t)
\end{aligned} \tag{2}$$

All components are implemented as multi-layer perceptrons (MLPs). The AFI module transforms the input observation o_t and associated deltas Δ_t into a high-order latent representation x_t^{HO} . The RSSM core updates the recurrent state h_t , while the encoder and dynamics predictor define a variational posterior and prior over discrete latent states z_t . We define patient state s_t is the concatenation of the stochastic state z_t and deterministic state h_t . The reward, continuation, and decoder heads generate task-specific outputs. Reward predictor learns to predict immediate rewards from latent features while the continuation predictor learns whether the trajectory ends. The decoder can reconstruct inputs from the latent space. Missing values in the input are masked during reconstruction, and their gradients are not propagated to avoid biased updates. We jointly train the full model by minimizing the following objective:

$$\mathcal{L}(\phi) \doteq \mathbb{E}_{q_\phi} \left[\sum_{t=1}^T (\beta_{\text{rew}} \mathcal{L}_{\text{rew}}(\phi) + \beta_{\text{con}} \mathcal{L}_{\text{con}}(\phi) + \beta_{\text{rec}} \mathcal{L}_{\text{rec}}(\phi) + \beta_{\text{dyn}} \mathcal{L}_{\text{dyn}}(\phi) + \beta_{\text{rep}} \mathcal{L}_{\text{rep}}(\phi)) \right] \tag{3}$$

3.2 Policy Learning via Latent Imagination

By leveraging the trained world model, we employ RL to learn an effective treatment policy using a two-phased learning strategy. To clarify our setup, we distinguish the concepts of imagination through time and imagination through horizon. Here, imagining through time means the sole continuation of a single patient trajectory given historical states while imagining through horizon means the planning horizon starting from each distinct state on that trajectory. (Figure 1)

3.2.1 Phase 1: Imagine through Time

The RL agent learns an initial policy from retrospective clinical data with few steps imagined in the time space. This phase prioritizes grounding the policy in past patient histories to ensure stability and alignment with real-world clinical patterns. For each real patient trajectory, we imagine $\tau = 10$ future steps in latent space. Given the last posterior state as s_T , the world model and actor continue the trajectory by predicting $s_{T+1:T+\tau}$, actions $a_{T+1:T+\tau}$ forming a hybrid rollout as $s_{\text{hybrid}} = [s_{1:T}, s_{T+1:T+\tau}]$. The critic predicts the distribution of returns, and we use the expected value of the predicted distribution at each state s_t $v_t \doteq \mathbb{E}[v_\psi(\cdot | s_t)]$ for bootstrapping. We compute bootstrapped λ -returns using the reward and continue predictor for both real and imagined states to keep the reward scale stable and the critic is trained using the maximum likelihood:

$$\mathcal{L}_{\text{critic}}(\psi) \doteq - \sum_{t=1}^{T+\tau} \ln p_\psi(R_t^\lambda | s_t) \quad R_t^\lambda \doteq \hat{r}_t + \gamma((1-\lambda)v_t + \lambda R_{t+1}^\lambda) \quad R_{T+\tau}^\lambda \doteq v_{T+\tau} \tag{4}$$

3.2.2 Phase 2: Imagine through Horizon

In Phase 2, the policy learned in Phase 1 is refined using fully imagined trajectories generated by the world model. For each state starting from $t = 0$, the model imagines $H = 15$ future steps. The initial batch and time dimensions are flattened to accelerate training, and imagination proceeds along the additional horizon dimension H (see Figure 1(b)). This encourages learning from diverse starting points and partial contexts, enabling the policy to explore different clinical stages. Since the recommendations are now less tied to historical data, Phase 2 enables out-of-distribution robustness. We now only update loss on the imagined steps:

$$\mathcal{L}_{\text{critic}}(\psi) \doteq - \sum_{t=1}^H \ln p_\psi(R_t^\lambda | s_t) \quad R_t^\lambda \doteq \hat{r}_t + \gamma((1-\lambda)v_t + \lambda R_{t+1}^\lambda) \quad R_H^\lambda \doteq v_H \tag{5}$$

4 Experiments

4.1 Datasets

For the sepsis treatment, we used the popular MIMIC-IV [16], extracting 21,233 adult septic patients. In line with prior work, we excluded patients without mortality outcomes, those with treatment withdrawal or multiple ICU stays. Each trajectory started at the later of ICU admission or 24 hours before diagnosis, and ended at the earliest of 48 hours post-diagnosis, ICU discharge, or death. Each observation included 40 physiological features, and the outcome is 90-day mortality.

For MV management, we used the eICU Collaborative Research (eICU)[33] database, and extracted patients aged ≥ 16 who received MV for at least 24 hours. Following the literature, we excluded patients missing mortality, height, or gender data, those ventilated for >14 days, and those with missing PEEP, FiO₂, and tidal volume records. After filtering, 21,595 patients were retained. Each observation included 41 physiological features, and the outcome is hospital mortality. See Appendix C.1: Datasets for the full list of features, feature selection process and action discretization.

4.2 Baselines

We evaluate MedDreamer against a range of model-based and model-free RL baselines, as well as the clinician policy derived from the actions recorded in historical EHR data.

Model-based baselines: (1) *MBRL-BNN* [35] is a fully model-based method that uses a Bayesian Neural Network to model patient dynamics for sepsis treatment. Although foundational, it does not address irregular sampling or generalize beyond a single task. (2) *DreamerV3* [?] is a recent model-based algorithm based on latent imagination. We adapt it to clinical settings as a strong general-purpose baseline. (3) *MBRL-EHR* [22] is a hybrid method that uses offline EHR data as a surrogate world model for glucose control in DKA patients. While not fully model-based, it incorporates model-based components and is included for comparison.

Model-free baselines: (4) *DDQN* [34] is a foundational model-free RL method for sepsis treatment. (2) *EZ-Vent* [24] and (3) *DeepVent* [19] are offline RL methods developed for MV management, based on Batch-Constrained Q-Learning (BCQ) and Conservative Q-Learning (CQL), respectively.

Since most prior work is task-specific (i.e., DDQN and MBRL-BNN for sepsis, and EZ-Vent and DeepVent for ventilation), we included baselines relevant to both the tasks. All models are evaluated on two benchmark datasets, MIMIC for sepsis and eICU for ventilation, and results are averaged over five random seeds.

See Appendix C.2: Baselines for baseline configurations, and Appendix C.4: Training Details and Hyperparameters for details on the loss functions, model architectures, and other hyperparameters.

4.3 Evaluation Metrics

We comprehensively evaluate all models on both sepsis treatment and mechanical ventilation management using a combination of quantitative and qualitative metrics to assess clinical efficacy and alignment with real-world clinical outcomes as follows (see Appendix C.3: Evaluation Metrics for more details on these metrics):

Quantitative Metrics: (1) *Relative Mortality (RM)*: Measures improvement over real-world clinical policy using $(EM-CM)/CM$, where EM is the estimated mortality under the learned policy and CM is clinician mortality. Higher RM indicates greater mortality reduction. (2) *Episode Return*: Sum of predicted rewards over patient trajectories, indicating treatment efficacy. For imagined trajectories, rewards were collected from full latent rollouts, whereas for real trajectories, the policy was applied step-by-step. All returns were computed from the learned reward model for consistency. (3) *Off-Policy Evaluation (OPE) Metrics*: Importance weighted return estimator (V_CWPDIS) evaluates the quality of the policy from historical data, and Effective Sample Size (ESS) measures the stability and reliability of V_CWPDIS estimates. Effective policies indicate high V_CWPDIS and ESS values.

Qualitative Analyses: (4) *Mortality vs Expected Return*: Examines whether higher policy returns correspond to lower observed mortality, ensuring clinical validity. (5) *Action Distribution*: Visualizes the range and frequency of treatment actions, assessing the plausibility and alignment of clinician

Table 1: Relative Mortality (RM) across models for Sepsis treatment and MV Management.

	Sepsis - RM(%)	MV - RM(%)
EZ-Vent[24]	4.99	14.33
DeepVent[19]	3.49	11.87
DDQN[34]	-0.49	-10.56
MBRL-BNN[35]	16.07	4.14
MBRL-EHR[22]	-2.05	-21.13
DreamerV3[13]	8.69	13.70
MedDreamer	20.86	16.00

practices. (6) *Mortality vs Action Difference*: Measures the divergence between policy and clinician actions, and its correlation with patient mortality.

4.4 Results and Discussion

Comparison of Relative Mortality: Table 1 presents the RM values for each model for both tasks. Most models perform better on the specific tasks they were originally designed for. For example, MBRL-BNN underperformed on MV task, despite being competitive on sepsis. Similarly, EZ-vent and DeepVent performed better under MV management, and underperformed in sepsis. Furthermore, MBRL-EHR, originally developed for blood glucose control in DKA patients, and DDQN, a generic RL baseline failed to outperform clinician policy on both tasks, showing negative RM values. DreamerV3 showed relatively balanced performance, with moderate RM across both tasks, showcasing some generalization ability, unlike other baselines. However, it failed to outperform MBRL-BNN under sepsis. In contrast, MedDreamer achieved the highest RM under each task, improving upon the next-best baseline by 4.79% on sepsis (compared to MBRL-BNN), and 2.3% on MV (compared to DreamerV3), showcasing its robustness and clinical effectiveness across diverse treatment settings. We attribute MedDreamer’s performances to several key design choices. Unlike previous baselines that relied on coarse discretization and imputation that lead to losing important temporal signals, MedDreamer explicitly models irregular, high-frequency data directly, modeling realistic patient dynamics in a structured latent space. Moreover, the two-phase training helps decouple world model and policy learning, avoiding the early instability often observed in DreamerV3’s joint training, leading to more stable convergence and improved mortality outcomes.

Accuracy of the World Model: To assess the model accuracy, we evaluate its ability to reconstruct physiological signals and capture clinically meaningful patterns related to patient outcomes. Figure 2 compares the original mean blood pressure (MBP) values to those generated by our world model, averaged per step across randomly selected 50 trajectories. The close alignment over time between the reconstructed and true MBP demonstrates that our world model can accurately capture and reproduce fine-grained physiological signals. A small divergence appears in longer-term predictions, which is expected due to trajectory length variability and increased in high instability in later clinical stages. Figure 3 illustrates the relationship between estimated mortality and episode return, computed using

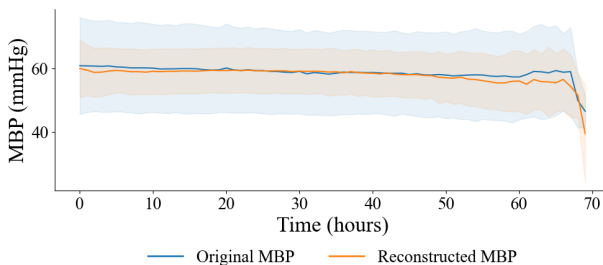


Figure 2: Original and reconstructed mean blood pressure (MBP), averaged over 50 trajectories.

the reward predictor to ensure fair and consistent evaluation. Compared to clinicians, our model showed better risk stratification by consistently assigning lower returns to higher-mortality cases and vice versa, for both sepsis and MV tasks. The steeper negative slope indicates that the model

captures meaningful latent representations that align with mortality outcomes. See Appendix D.6 for additional results on AI episode returns per transition in historical data.

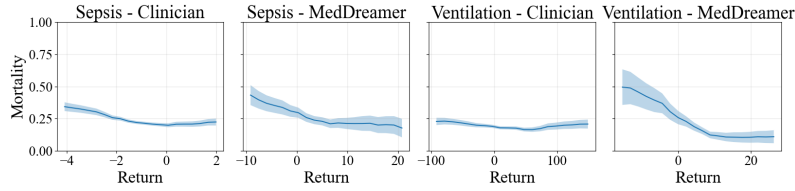


Figure 3: Mortality vs return, showing MedDreamer’s ability to assign lower returns to higher risk.

Effectiveness of Phase 1 - Training through Time: We evaluate MedDreamer Phase 1 using the standard Offline Policy Evaluation (OPE) metrics (V_CWPDIS and ESS). These metrics are suitable for Phase 1, which largely relies on real data. Figure 4 shows that when training progresses, both metrics increase steadily, indicating improved return estimates and evaluation stability. MedDreamer converges within 2000 epochs and consistently outperforms model-free and model-based baselines across both tasks, indicating better policy-alignment and higher returns. In contrast, other model-based baselines show limited improvement, and notably DreamerV3 struggles to converge due to instability in joint end-to-end training.

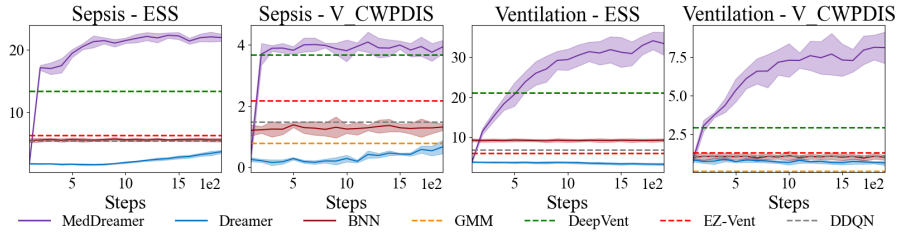


Figure 4: V_CWPDIS and ESS over training steps, showing policy return estimates and evaluation reliability during Phase 1.

Effectiveness of Phase 2 - Training through Horizon: Phase 2 refines the learned policy using imagined rollouts. During testing, each trajectory begins from a real state at step 5, and imagines 50 future steps using the learned world model. Episode return is computed by adding the generated rewards across the imagined horizon. As shown in Figure 5, compared to phase 1, phase 2 considerably improves the imagined episode returns across both tasks. This improvement stems from training the policy to imagine from multiple mid-trajectory states, allowing richer exploration and better long-term optimization. The high return gap between phase 1 and 2 highlights the benefit of imagination beyond the episode endpoints used in phase 1.

Clinically Meaningful Decision-Making: The Sequential Organ Failure Assessment (SOFA) score is a widely used clinical metric in sepsis care to assess organ dysfunction, where higher scores

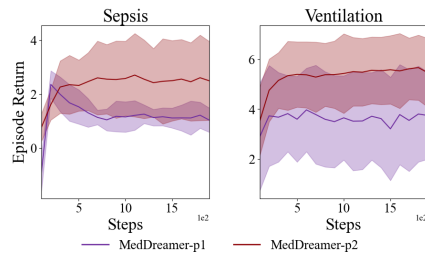


Figure 5: Episode return from imagined rollouts starting at step 5. Phase 2 (MedDreamer-p2) significantly improves long-term return over Phase 1 (MedDreamer-p1) in both sepsis and ventilation tasks, demonstrating enhanced planning from mid-trajectory states.

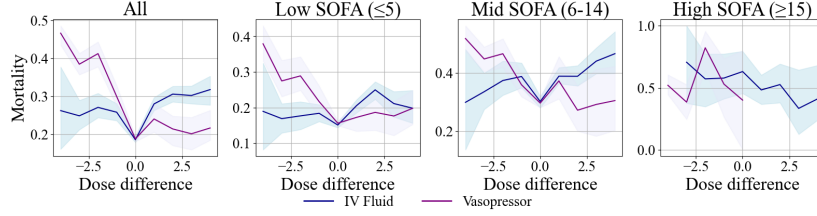


Figure 6: Difference between clinician and policy predicted action vs mortality stratified by SOFA.

indicate increased mortality risk. We observe the policy behavior across varying clinical severities by categorizing the patient into 4 SOFA ranges: Low (≤ 5), Mid (6-14), High (≥ 15), and All. Figure 6 shows the difference in recommended dosages between the policy and clinicians, and corresponding mortality. Except for high SOFA, all groups show a distinct V-shaped pattern, where mortality is lowest when the policy aligns with clinician decisions (i.e., $x=0$) and increases in divergence when in either direction. High SOFA exhibits less consistent patterns, reflecting increased complexity and variability of treating severe patients, where clinical decisions are more uncertain. This could also be due to the fact that current practices in high-acuity sepsis settings is known to be suboptimal.

Table 2: Ablation study results.

	ESS	V_CWPDIS
NoAFI	20.92	4.52
P1-RL	17.75	4.11
P1-NoIm	17.81	4.63
$\tau=10$	22.88	4.75
$\tau=30$	21.23	4.31
$\tau=50$	19.97	4.45

Ablation Studies: For comprehensive validation, we conducted three ablation studies (see Table 7) as follows. (1) *Role of AFI in Handling Sparse and Irregular Data:* To assess the role of the AFI module in handling missing and irregular EHR data, we compare MedDreamer to a variant without the AFI (MD-NoAFI), where missing values are imputed using nearest-neighbor fill. Removing AFI leads to a drop in both ESS and V_CWPDIS (8.95% and 4.96%), indicating that AFI plays a critical role in extracting meaningful dynamics from sparse and irregular EHR data. (2) *Balancing Real and Imagined Rollouts:* we examine the importance of Phase 1 imagination by comparing its design with 2 variants: one trained with only replay loss (MD-P1-RL) and another using posteriors without imagined steps (MD-P1-NoIm). Both decreased performance indicating the value of early exposure to partial imagination to enrich policy learning and mitigating distributional mismatch. (3) *Importance of Early Imagination:* We evaluated the impact of varying the imagined to total steps ratio ($\tau = 10, 30, 50$) during training. Best performance is observed with $\tau = 10$, with decreasing performance with higher values. This suggests that a moderate number of imagined transitions is key to balance realism and foresight, preventing drift from true dynamics.

See Appendix D: Evaluation for additional results, including the choice of world model, mortality trends during training, clinician vs. MedDreamer policies, Phase 1 policy training choice, and more. See Appendix F: Limitations for key assumptions and constraints. The anonymized code to reproduce all experiments is available at: <https://anonymous.4open.science/r/MedDreamer-615C/>.

5 Conclusion

We introduced MedDreamer, a two-phased model-based RL framework for personalized treatment recommendation from complex clinical data. To address sparsity and irregularity, we proposed an Adaptive Feature Integration (AFI) module and trained a structured latent world model. Our two-phase pipeline helps ground the policy in real clinical trajectories and further enhance its robustness with imagination-based exploration. Extensive experiments on sepsis and ventilation tasks show that MedDreamer effectively handles complex EHR data, improves generalization, and considerably reduces estimated mortality, demonstrating its potential as a reliable clinical decision support system.

References

- [1] Hassan Ali. Reinforcement learning in healthcare: optimizing treatment strategies, dynamic resource allocation, and adaptive clinical decision-making. *Int J Comput Appl Technol Res*, 11(3):88–104, 2022.
- [2] Ali Amirahmadi, Mattias Ohlsson, and Kobra Etminani. Deep learning prediction models based on ehr trajectories: A systematic review. *Journal of biomedical informatics*, 144:104430, 2023.
- [3] Marc G Bellemare, Will Dabney, and Rémi Munos. A distributional perspective on reinforcement learning. In *International conference on machine learning*, pages 449–458. PMLR, 2017.
- [4] Yoshua Bengio, Aaron Courville, and Pascal Vincent. Representation learning: A review and new perspectives. *IEEE transactions on pattern analysis and machine intelligence*, 35(8):1798–1828, 2013.
- [5] Maxime Burchi and Radu Timofte. Learning transformer-based world models with contrastive predictive coding. *arXiv preprint arXiv:2503.04416*, 2025.
- [6] Shaotao Chen, Xihe Qiu, Xiaoyu Tan, Zhijun Fang, and Yaochu Jin. A model-based hybrid soft actor-critic deep reinforcement learning algorithm for optimal ventilator settings. *Information sciences*, 611:47–64, 2022.
- [7] Fei Deng, Junyeong Park, and Sungjin Ahn. Facing off world model backbones: Rnns, transformers, and s4. *Advances in Neural Information Processing Systems*, 36:72904–72930, 2023.
- [8] Adrian Goldwaser and Michael Thielscher. Deep reinforcement learning for general game playing. In *Proceedings of the AAAI conference on artificial intelligence*, volume 34, pages 1701–1708, 2020.
- [9] David Ha and Jürgen Schmidhuber. World models. *arXiv preprint arXiv:1803.10122*, 2018.
- [10] Danijar Hafner, Timothy Lillicrap, Jimmy Ba, and Mohammad Norouzi. Dream to control: Learning behaviors by latent imagination. *arXiv preprint arXiv:1912.01603*, 2019.
- [11] Danijar Hafner, Timothy Lillicrap, Ian Fischer, Ruben Villegas, David Ha, Honglak Lee, and James Davidson. Learning latent dynamics for planning from pixels. In *International conference on machine learning*, pages 2555–2565. PMLR, 2019.
- [12] Danijar Hafner, Timothy Lillicrap, Mohammad Norouzi, and Jimmy Ba. Mastering atari with discrete world models. *arXiv preprint arXiv:2010.02193*, 2020.
- [13] Danijar Hafner, Jurgis Pasukonis, Jimmy Ba, and Timothy Lillicrap. Mastering diverse domains through world models, 2024. URL <https://arxiv.org/abs/2301.04104>.
- [14] Christina X Ji, Michael Oberst, Sanjat Kanjilal, and David Sontag. Trajectory inspection: A method for iterative clinician-driven design of reinforcement learning studies. *AMIA Summits on Translational Science Proceedings*, 2021:305, 2021.
- [15] Yan Jia, John Burden, Tom Lawton, and Ibrahim Habli. Safe reinforcement learning for sepsis treatment. In *2020 IEEE International conference on healthcare informatics (ICHI)*, pages 1–7. IEEE, 2020.
- [16] Alistair Johnson, Lucas Bulgarelli, Tom Pollard, Steven Horng, Leo Anthony Celi, and Roger Mark. Mimic-iv. *PhysioNet*. Available online at: <https://physionet.org/content/mimiciv/1.0/>(accessed August 23, 2021), pages 49–55, 2020.
- [17] Kia Khezeli, Scott Siegel, Benjamin Shickel, Tezcan Ozrazgat-Baslanti, Azra Bihorac, and Parisa Rashidi. Reinforcement learning for clinical applications. *Clinical Journal of the American Society of Nephrology*, 18(4):521–523, 2023.

- [18] Matthieu Komorowski, Leo A Celi, Omar Badawi, Anthony C Gordon, and A Aldo Faisal. The artificial intelligence clinician learns optimal treatment strategies for sepsis in intensive care. *Nature medicine*, 24(11):1716–1720, 2018.
- [19] Flemming Kondrup, Thomas Jiralerspong, Elaine Lau, Nathan de Lara, Jacob Shkrob, My Duc Tran, Doina Precup, and Sumana Basu. Towards safe mechanical ventilation treatment using deep offline reinforcement learning. In *Proceedings of the AAAI Conference on Artificial Intelligence*, volume 37, pages 15696–15702, 2023.
- [20] Simon Lambden, Pierre Francois Laterre, Mitchell M Levy, and Bruno Francois. The sofa score—development, utility and challenges of accurate assessment in clinical trials. *Critical Care*, 23:1–9, 2019.
- [21] Sergey Levine, Chelsea Finn, Trevor Darrell, and Pieter Abbeel. End-to-end training of deep visuomotor policies. *Journal of Machine Learning Research*, 17(39):1–40, 2016.
- [22] Tianhao Li, Zhishun Wang, Wei Lu, Qian Zhang, and Dengfeng Li. Electronic health records based reinforcement learning for treatment optimizing. *Information Systems*, 104:101878, 2022.
- [23] Andrew C Liu, Krishna Patel, Ramya Dhatri Vunikili, Kipp W Johnson, Fahad Abdu, Shivani Kamath Belman, Benjamin S Glicksberg, Pratyush Tandale, Roberto Fontanez, Oommen K Mathew, et al. Sepsis in the era of data-driven medicine: personalizing risks, diagnoses, treatments and prognoses. *Briefings in Bioinformatics*, 21(4):1182–1195, 2020.
- [24] Siqi Liu, Qianyi Xu, Zhuoyang Xu, Zhuo Liu, Xingzhi Sun, Guotong Xie, Mengling Feng, and Kay Choong See. Reinforcement learning to optimize ventilator settings for patients on invasive mechanical ventilation: Retrospective study. *Journal of Medical Internet Research*, 26:e44494, 2024.
- [25] Xiangyu Liu, Chao Yu, Qikai Huang, Luhao Wang, Jianfeng Wu, and Xiangdong Guan. Combining model-based and model-free reinforcement learning policies for more efficient sepsis treatment. In *Bioinformatics Research and Applications: 17th International Symposium, ISBRA 2021, Shenzhen, China, November 26–28, 2021, Proceedings 17*, pages 105–117. Springer, 2021.
- [26] MingYu Lu, Zachary Shahn, Daby Sow, Finale Doshi-Velez, and H Lehman Li-wei. Is deep reinforcement learning ready for practical applications in healthcare? a sensitivity analysis of duel-ddqn for hemodynamic management in sepsis patients. In *AMIA Annual Symposium Proceedings*, volume 2020, page 773, 2021.
- [27] Zhiyao Luo, Yangchen Pan, Peter Watkinson, and Tingting Zhu. Reinforcement learning in dynamic treatment regimes needs critical reexamination. *arXiv preprint arXiv:2405.18556*, 2024.
- [28] Volodymyr Mnih, Koray Kavukcuoglu, David Silver, Alex Graves, Ioannis Antonoglou, Daan Wierstra, and Martin Riedmiller. Playing atari with deep reinforcement learning. 2013. URL <http://arxiv.org/abs/1312.5602>. cite arxiv:1312.5602Comment: NIPS Deep Learning Workshop 2013.
- [29] Mila Nambiar, Supriyo Ghosh, Priscilla Ong, Yu En Chan, Yong Mong Bee, and Pavitra Krishnaswamy. Deep offline reinforcement learning for real-world treatment optimization applications. In *Proceedings of the 29th ACM SIGKDD Conference on Knowledge Discovery and Data Mining*, pages 4673–4684, 2023.
- [30] Peter C Nauka, Jason N Kennedy, Emily B Brant, Matthieu Komorowski, Romain Pirracchio, Derek C Angus, and Christopher W Seymour. Challenges with reinforcement learning model transportability for sepsis treatment in emergency care. *npj Digital Medicine*, 8(1):1–5, 2025.
- [31] Zhenghao Peng, Wenjie Luo, Yiren Lu, Tianyi Shen, Cole Gulino, Ari Seff, and Justin Fu. Improving agent behaviors with rl fine-tuning for autonomous driving. In *European Conference on Computer Vision*, pages 165–181. Springer, 2024.

- [32] Dilruk Perera, Siqi Liu, Kay Choong See, and Mengling Feng. Smart imitator: Learning from imperfect clinical decisions. *Journal of the American Medical Informatics Association*, page ocae320, 01 2025. ISSN 1527-974X. doi: 10.1093/jamia/ocae320. URL <https://doi.org/10.1093/jamia/ocae320>.
- [33] Tom J Pollard, Alistair EW Johnson, Jesse D Raffa, Leo A Celi, Roger G Mark, and Omar Badawi. The eicu collaborative research database, a freely available multi-center database for critical care research. *Scientific data*, 5(1):1–13, 2018.
- [34] Aniruddh Raghu, Matthieu Komorowski, Imran Ahmed, Leo Celi, Peter Szolovits, and Marzyeh Ghassemi. Deep reinforcement learning for sepsis treatment. *arXiv preprint arXiv:1711.09602*, 2017.
- [35] Aniruddh Raghu, Matthieu Komorowski, and Sumeetpal Singh. Model-based reinforcement learning for sepsis treatment. *arXiv preprint arXiv:1811.09602*, 2018.
- [36] Mohammad Reza Samsami, Artem Zholus, Janarthanan Rajendran, and Sarath Chandar. Mastering memory tasks with world models. *arXiv preprint arXiv:2403.04253*, 2024.
- [37] Julian Schrittwieser, Ioannis Antonoglou, Thomas Hubert, Karen Simonyan, Laurent Sifre, Simon Schmitt, Arthur Guez, Edward Lockhart, Demis Hassabis, Thore Graepel, et al. Mastering atari, go, chess and shogi by planning with a learned model. *Nature*, 588(7839):604–609, 2020.
- [38] Timo Spinde, Jan-David Krieger, Terry Ruas, Jelena Mitrović, Franz Götz-Hahn, Akiko Aizawa, and Bela Gipp. Exploiting transformer-based multitask learning for the detection of media bias in news articles. In *International conference on information*, pages 225–235. Springer, 2022.
- [39] István Szita. *Reinforcement Learning in Games*, pages 539–577. Springer Berlin Heidelberg, Berlin, Heidelberg, 2012. ISBN 978-3-642-27645-3. doi: 10.1007/978-3-642-27645-3_17. URL https://doi.org/10.1007/978-3-642-27645-3_17.
- [40] Chen Tang, Ben Abbatematteo, Jiaheng Hu, Rohan Chandra, Roberto Martín-Martín, and Peter Stone. Deep reinforcement learning for robotics: A survey of real-world successes. In *Proceedings of the AAAI Conference on Artificial Intelligence*, volume 39, pages 28694–28698, 2025.
- [41] Jianxun Wang, David Roberts, and Andinet Enquobahrie. Inferring continuous treatment doses from historical data via model-based entropy-regularized reinforcement learning. In *Asian Conference on Machine Learning*, pages 433–448. PMLR, 2020.
- [42] Ronald J Williams. Simple statistical gradient-following algorithms for connectionist reinforcement learning. *Machine learning*, 8(3-4):229–256, 1992.
- [43] Yaodong Yang and Jun Wang. An overview of multi-agent reinforcement learning from game theoretical perspective. *arXiv preprint arXiv:2011.00583*, 2020.
- [44] Chao Yu, Jiming Liu, Shamim Nemati, and Guosheng Yin. Reinforcement learning in healthcare: A survey. *ACM Computing Surveys (CSUR)*, 55(1):1–36, 2021.
- [45] Tianhe Yu, Garrett Thomas, Lantao Yu, Stefano Ermon, James Y Zou, Sergey Levine, Chelsea Finn, and Tengyu Ma. Mopo: Model-based offline policy optimization. In H. Larochelle, M. Ranzato, R. Hadsell, M.F. Balcan, and H. Lin, editors, *Advances in Neural Information Processing Systems*, volume 33, pages 14129–14142. Curran Associates, Inc., 2020. URL https://proceedings.neurips.cc/paper_files/paper/2020/file/a322852ce0df73e204b7e67cbbef0d0a-Paper.pdf.
- [46] Tianhe Yu, Aviral Kumar, Rafael Rafailov, Aravind Rajeswaran, Sergey Levine, and Chelsea Finn. Combo: Conservative offline model-based policy optimization. *Advances in neural information processing systems*, 34:28954–28967, 2021.
- [47] Tianyi Zhang, Yimeng Qu, Deyong Wang, Ming Zhong, Yunzhang Cheng, and Mingwei Zhang. Optimizing sepsis treatment strategies via a reinforcement learning model. *Biomedical Engineering Letters*, 14(2):279–289, 2024.

Appendix

A Ethical Statement

The collection of patient information and creation of the research resource in the MIMIC-IV database was reviewed by the Institutional Review Board at the Beth Israel Deaconess Medical Center (number 2001-P-001699/14), which granted a waiver of informed consent and approved the data-sharing initiative. For the eICU database, it has been approved by the Institutional Review Board of the Massachusetts Institute of Technology. After completing the National Institutes of Health’s online training course and the Protection of Human Research Participants Examination, we had the access to extract data from both the MIMIC-IV and the eICU databases. The study data are anonymous and deidentified. Our proposed method is designed solely to assist clinicians in their decision-making process by providing data-driven insights and recommendations. The final treatment decisions remain entirely under the control of the clinicians, ensuring that their expertise and judgment guide patient care. Importantly, all models were trained and tested using publicly available retrospective datasets, ensuring that no live patient data or clinical trials were involved in the development process. This approach aligns with established ethical standards, minimizing potential risks and maintaining the highest level of transparency and safety.

B Reward Design

For sepsis treatment task, in line with the literature[34, 18], we combined the terminal reward together with the intermediate reward calculated based on the sofa scores and lactate level changes. Although we avoid imputing input features (o_t), we selectively impute missing values for reward-critical variables. For the SOFA scores missing in the sepsis task, SOFA scores are computed using existing features following the guideline[20], and missing lactate values are imputed using K-nearest neighbors (KNN) with $k=5$. The overall reward function was defined as follows:

$$\begin{aligned} R_{\text{im}}^{\text{Sep}}(s_t, s_{t+1}) = & C_0(s_{t+1}^{\text{SOFA}} = s_t^{\text{SOFA}} \wedge s_{t+1}^{\text{SOFA}} > 0) \\ & + C_1(s_{t+1}^{\text{SOFA}} - s_t^{\text{SOFA}}) \\ & + C_2 \tanh(s_{t+1}^{\text{lactate}} - s_t^{\text{lactate}}) \end{aligned} \quad (6)$$

For ventilation, we impute by filling using the nearest values for SpO₂ and MBP. We follow the same reward design in[24] where intermediate rewards support SpO₂ and MBP values to be within clinically optimal ranges:

$$\begin{aligned} R_{\text{im}}^{\text{Vent}}(s_t, s_{t+1}) = & b \cdot \left(\mathbb{1}_{[94 \leq s_{t+1}^{\text{SpO}_2} \leq 98]} - \frac{1}{2} \cdot \mathbb{1}_{[s_{t+1}^{\text{SpO}_2} < 94 \vee s_{t+1}^{\text{SpO}_2} > 98]} \right) \\ & + c \cdot \left(\mathbb{1}_{[70 \leq s_{t+1}^{\text{MBP}} \leq 80]} - \frac{1}{2} \cdot \mathbb{1}_{[s_{t+1}^{\text{MBP}} < 70 \vee s_{t+1}^{\text{MBP}} > 80]} \right) \end{aligned} \quad (7)$$

The full reward function integrates intermediate and terminal outcomes as follows:

$$R(s_t, s_{t+1}) = \begin{cases} +R_r, & \text{if } s_{t+1} \in S_T \cap S_{\text{sur}} \\ -R_r, & \text{if } s_{t+1} \in S_T \cap S_{\text{dec}} \\ R_{\text{im}}(s_t, s_{t+1}), & \text{if } s_{t+1} \notin S_T \end{cases} \quad (8)$$

C Experimental Setup and Datasets

RL is widely applied in domains such as robotics, games and autonomous driving. In the context of treatment recommendation, the fundamental components of RL can be mapped to key clinical decision-making aspects as follows.

Observation and state (o_t): At each time t , the agent receives an observation o_t which includes raw clinical features such as patient demographics, vital signs, lab tests and other biomarkers[17, 26].

Action (a_t): The action represents clinical interventions at each time step. These actions are defined based on the treatment domain. For example, IV fluids and vasopressors for sepsis management[?], and FiO₂, PEEP, and tidal volume for ventilation treatment[24].

Table 3: List of sepsis features.

Category	Feature Name
Demographics (5)	Age, Gender, Weight, Readmission, Elixhauser Score
Vital signs (12)	Heart Rate, SBP, MBP, DBP, Respiratory rate, Temperature, SpO ₂ , Shock Index, SOFA, GCS, FiO ₂ , SIRS
Lab values (22)	Lactate, PaO ₂ , PaCO ₂ , pH, Base excess, CO ₂ , PaO ₂ /FiO ₂ , WBC, Platelet, BUN, Creatinine, PTT, PT, INR, AST, ALT, Total Bilirubin, Magnesium, Ionized Calcium, Calcium, Urine Output, Mechanical Ventilation
Other (1)	Step ID

Abbreviations - INR: International normalized ratio; PT: Prothrombin time; PTT: Partial thromboplastin time; SIRS: Systemic inflammatory response syndrome; WBC: White blood cell; GCS: Glasgow coma scale; SBP: Systolic blood pressure; MBP: Mean blood pressure; DBP: Diastolic blood pressure; SOFA: Sequential organ failure assessment; SpO₂: Peripheral oxygen saturation; FiO₂: Fraction of inspired oxygen; PaO₂: Partial pressure of oxygen; PaCO₂: Partial pressure of carbon dioxide; PaO₂/FiO₂: Arterial oxygen partial pressure to fractional inspired oxygen ratio; BUN: Blood urea nitrogen; AST: Aspartate aminotransferase; ALT: Alanine aminotransferase.

C.1 Datasets

We extract 21,233 septic patients who are 18 years old and above from the popular MIMIC-IV database [16]. We exclude those patients whose mortality was not documented or had withdraw of treatment and only kept the first ICU stay of the patient. Each trajectory start is set at the suspected sepsis infection time (i.e., 24 hours before diagnosis) or the ICU admission time, whichever was later. End time was set to 48 hours after diagnosis or the time of death/discharge, whichever was earlier. We filter out patients who miss SOFA or lactate values for the whole trajectory for better reward modeling. The observations contain 40 physiological measurements including demographics, vital signs, and laboratory test results listed in Table3. We use 90 day mortality as the final outcome following previous work[18]. For the action space, two interventions are included IV fluids and vasopressors. We discretize the dosage of each treatment into four quantile bins along with a no-treatment option, resulting in five discrete levels per treatment. Consequently, the joint action space consists of $5 \times 5 = 25$ possible treatment combinations.

We conduct ventilation task on eICU Collaborative Research (eICU)[33] database. We include patients who are at least 16 years old and receive mechanical ventilation for a minimum duration of 24 hours. Only the first ICU admission is considered for each patient, and we focus on the first 48 hours of ventilation data. We exclude patients who have missing values for hospital mortality, height, or gender, or if any of these variables are entirely absent throughout their recorded trajectory. We also exclude patients who lack records for key ventilatory settings—positive end-expiratory pressure (PEEP), fraction of inspired oxygen (FiO₂), and tidal volume—throughout the entire ventilation period. To ensure clinical relevance, we further exclude patients whose total duration of mechanical ventilation exceeds 14 days, as these cases typically involve long-term support and may not be representative of the general mechanically ventilated population. After applying all exclusion criteria, 21,595 patients remain for analysis. The primary outcome of interest is hospital mortality. Table5 lists the 41 features selected for training. In our study, the action space is constructed as 18 possible discrete actions from combinations of low, medium, and high levels of the 3 ventilator settings: PEEP, FiO₂, and ideal body weight-adjusted tidal volume (summarized in Table4).

C.2 Baselines

We evaluated the proposed method against the following state-of-the-art model-free and model-based RL methods.

Table 4: Categorization of action levels for PEEP, FiO₂ and tidal volume.

Intervention	Category	Threshold
PEEP (cmH ₂ O)	Low	≤ 5
	High	> 5
FiO ₂ (%)	Low	< 35
	Medium	35–50
	High	≥ 50
Tidal Volume (ml/kg IBW)	Low	< 6.5
	Medium	6.5–8
	High	≥ 8

Table 5: List of MV features.

Category	Feature Name
Demographics (4)	Age, Gender, Admission Weight, Elixhauser Score
Vital signs (10)	Heart Rate, SBP, DBP, MBP, Respiratory Rate, Temperature, SpO ₂ , SIRS, SOFA, GCS
Lab values (27)	Richmond Agitation-Sedation Scale, Rate Std, Creatinine, Lactate, Bicarbonate, PaCO ₂ , pH, Base Excess, Chloride, Potassium, Sodium, Glucose, Hemoglobin, Ionized Calcium, Calcium, PTT, PT, INR, Platelet, WBC, Albumin, Magnesium, Analgesic and Sedative Medication Administration, Neuromuscular Blocking Agent Administration, ETCO ₂ , BUN, Urine Output

- **Clinician**: Actual clinician policy based on the actions given by the doctor in the historical data.
- **DDQN**[34]: A model-free approach for sepsis treatment based on DDQN.
- **DreamerV3**[13]: original dreamer algorithm trained simultaneously while updating the policy. The policy was optimized entirely on imagined trajectories generated by the learned world model.
- **MBRL-BNN**[35]: A model-based RL approach for sepsis treatment recommendation. It used Bayesian Neural Network to model the patient dynamics, learned the clinician’s policy using behavior cloning and then finetuned with REINFORCE[42].
- **MBRL-EHR**[22]: A model-based deep Q-learning framework for optimizing treatment strategies using electronic health records (EHRs), with a focus on blood glucose control in diabetic ketoacidosis (DKA) patients.
- **EZ-Vent**[24]: An offline RL system trained using Batch-Constrained Q-learning (BCQ) to optimize ventilator settings. The model uses time-varying intervals triggered by clinical deterioration to better align with real-world decision-making.
- **DeepVent**[19]: A decision support tool that applied Conservative Q-Learning (CQL) to recommend safe and effective mechanical ventilation settings, emphasized robustness to out-of-distribution (OOD) states and improved patient safety as key advantages of CQL.

C.3 Evaluation Metrics

Since treatment recommendation is an off-policy evaluation task, in line with the literature, we use the following off-policy evaluation metrics commonly used in healthcare RL:

- **V_CWPDIS:** Cumulative Weighted Per Decision Importance Sampling. We utilize off-policy evaluation metrics since directly executing the learned policy in real-ICU is impractical. V_CWPDIS estimates the expected return of a target policy by weighting rewards based on the alignment between the target and behavior policies while applying a discount factor to prioritize immediate rewards. The behavior policy is the clinician policy.
- **ESS:** We also calculate effective sampling size (ESS) to measure the number of effective samples contributing to the V_CWPDIS estimate, indicating the reliability and stability of the evaluation.
- **Mortality Rate:** The estimated mortality(EM) is calculated when executing the actions recommended by the trained policy by matching the return values from the plot. Relative mortality (RM) is calculated by comparing with the clinician mortality(CM) calculated based on retrospective data: $RM = (EM - CM)/CM$.

Additionally, we use the following qualitative metrics:

- **Episode Return:** We summed up the predicted reward of the trajectory for two cases, AI episode return is for per step prediction when we do a one-step action prediction for each prior state along a patient trajectories and get the reward under that action. We also calculated the accumulated rewards for the imagined trajectories as the imagined episode return.
- **Mortality vs Return:** A good policy should demonstrate a clear downward trend when it learns to associate high returns with low mortality. For model-free models, the returns are calculated using the expected return (e.g. Q values) and we consider the mortality to be the same for all the steps for the trajectory. While for model-based method, we use the episode return and plot that against the mortality of this trajectory.
- **Action Distribution:** The distribution of different action combinations.
- **Mortality vs Action Difference:** We calculate the difference of dosages for policy and clinician’s action and plot it against the mortality. The policy is good if when it aligns with clinician the mortality is low and when it diverge from clinician’s action the mortality is high (demonstrating a v-shape).

C.4 Training Details and Hyperparameters

All experiments are conducted on a single NVIDIA Tesla V100 GPU. For world model training, we use a batch size of 64, batch length of 50. We imagine for 10 steps for phase 1 and 15 steps for phase 2. All models use the same decoder, reward predictor, continue predictor and actor critic based on MLP with 2 hidden layers of size 512 with layer norm and a SiLU activation. The AFI module has an embedding size of 32. The dynamics model uses a GRU cell with a 256-dimensional hidden state and a stochastic latent space of size 32. The prior and posterior distributions over latent states are modeled as 32 categoricals, with minimum standard deviation of 0.3 and sigmoid activation with a range of 2 for standard deviation outputs. A learned initial hidden state is used to initialize each episode. The learning rate is 1×10^{-4} for world model and phase 1 policy training, 1×10^{-5} for phase 2 policy training.

Training losses for world model. For world model training, we adopt a suite of task-specific losses inspired by DreamerV3. \mathcal{L}_{rew} is a symlog-scaled two-hot encoding scheme, which discretizes the reward space into 255 buckets and computes a smooth approximation of log-likelihood using soft-assignment based on distance. This approach ensures stability across tasks with highly variable reward magnitudes. \mathcal{L}_{con} uses logistic regression and adopts a Bernoulli log-likelihood loss modeling whether the episode continues or terminates. To enhance robustness when decoding targets with large dynamic ranges or signed magnitudes, we adopt a symlog-based squared distance loss for \mathcal{L}_{rec} , defined as the squared difference between the predicted value and the symlog-transformed target. We also applied masks to \mathcal{L}_{rec} to make sure only the values that are not missing in the data are considered. The dynamics loss \mathcal{L}_{dyn} trains the sequence model to predict future latent states by minimizing the Kullback–Leibler (KL) divergence between the prior distribution $p_\phi(z_t | h_t)$ and the posterior distribution $q_\phi(z_t | h_t, x_t)$, which is conditioned on both history and current observations. Conversely, the representation loss \mathcal{L}_{rep} encourages the posterior to remain close to the prior, promoting the learning of latent features that are predictable through the model’s dynamics.

These two KL terms are computed with distinct gradient flows: one detaches the prior distribution, and the other detaches the posterior, thus directing optimization toward different model components. Each of the KL-based terms is clipped using free bits (with threshold 3), and the stop-gradient operator $\text{sg}(\cdot)$ is used to block gradients flowing into the target distributions. The dynamics and representation losses are scaled with coefficients $\beta_{\text{dyn}} = 0.5$ and $\beta_{\text{rep}} = 0.1$ respectively, as specified in the training configuration.

$$\begin{aligned}\mathcal{L}_{\text{dyn}}(\phi) &\doteq \max(1, \text{KL}[\text{sg}(q_\phi(z_t | h_t, x_t)) \| p_\phi(z_t | h_t)]) \\ \mathcal{L}_{\text{rep}}(\phi) &\doteq \max(1, \text{KL}[q_\phi(z_t | h_t, x_t) \| \text{sg}(p_\phi(z_t | h_t))])\end{aligned}\tag{9}$$

Training losses for policy. For actor-critic training, we compute actor loss $\mathcal{L}_{\text{actor}}$ using the REINFORCE algorithm [42]. We did not adopt the EMA regularization term as in DreamerV3 due to stability and showed the results in the ablation study. The loss is computed by sampling actions from the current policy and weighting their log-likelihoods by an advantage term, which is the difference between the predicted return and a baseline value function:

$$\mathcal{L}_{\text{actor}}(\theta) \doteq - \sum_{t=1}^T \text{sg}(R_t^\lambda - V_\psi(s_t)) \log \pi_\theta(a_t | s_t) + \eta \mathbb{H}[\pi_\theta(a_t | s_t)]\tag{10}$$

$\mathcal{L}_{\text{critic}}$ is computed using predicted λ -returns and a distributional value model trained by maximizing log-likelihood. To stabilize training, we maintain a slow-moving target value network \bar{V}_ψ , updated via exponential moving average with a fraction $\tau = 0.02$:

$$\mathcal{L}_{\text{critic}}(\psi) \doteq - \sum_{t=1}^T \ln p_\psi(R_t^\lambda | s_t) \quad R_t^\lambda \doteq \hat{r}_t + \gamma((1 - \lambda)v_t + \lambda R_{t+1}^\lambda) \quad R_T^\lambda \doteq v_T\tag{11}$$

Here we use T to represent the cases for both phase 1 and phase 2. We add a consistency loss to encourage agreement between the current and target value networks $\mathcal{L}_{\text{value}} += -\log p_\psi(\bar{V}_\psi(s_t))$. This acts as a regularizer that prevents rapid fluctuations in the critic and ensures smoother target estimation during policy optimization.

D Evaluation

D.1 Choice of World Model

To determine a suitable world model architecture for the clinical setting, we evaluated 2 additional DreamerV1 based frameworks: (1) DreamerV1-S, standard version which retains stochastic Gaussian latent variables, (2) DreamerV1-D, a fully deterministic version with no stochasticity in the latent space (see Table 6). These variants were used to especially explore the trade-offs between stochasticity and training stability in high-variance and sparse clinical data.

It was evident that DreamerV1-S struggled to capture the complex and noisy dynamics of patient trajectories. The use of continuous Gaussian latents makes it difficult to fit smooth distributions to highly variable transitions, leading to unstable training behavior. We considered DreamerV1-D to improve stability by replacing stochasticity with deterministic transitions. This led to improved stability in training but sacrifice the safety margin to produce robust results[11]. Both variants consistently produce low V_CWPDIS scores and RM and showed minimal improvement throughout training. Given these limitations, we adopt a DreamerV3-style stochastic recurrent state-space model for MedDreamer. This architecture provides a better balance between expressiveness, uncertainty modeling, and training stability. Its capacity to represent uncertainty more robustly makes it well-suited to the stochastic and complex nature of clinical environments.

Table 6: OPE metrics to evaluate DreamerV1 based framework.

Model	CWPDIS	RM(%)
DreamerV1-S	-1.34	0.14
DreamerV1-D	0.36	0.36
MedDreamer	4.75	20.86

D.2 Mortality Trends Across Training Steps

To assess the stability and effectiveness of policy learning over time, we track the estimated mortality produced by policies trained at different steps for both MedDreamer and DreamerV3. As shown in Figure7, MedDreamer exhibits a downward trend in estimated mortality as training progresses, indicating consistent policy improvement and effective learning from simulated experience. In contrast, DreamerV3 shows an upward trend in estimated mortality. This upward trend suggests that DreamerV3 exhibits significant instability, particularly during the early stages of training, and that its end-to-end training paradigm proves inefficient for our clinical data.

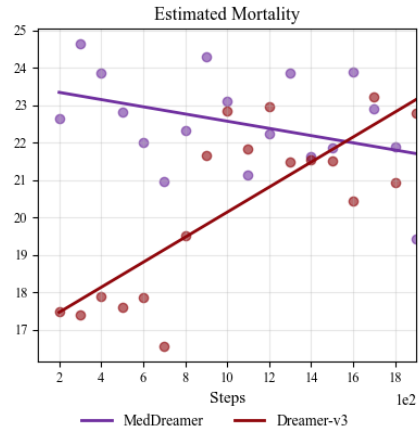


Figure 7: Estimated mortality as a function of training steps for MedDreamer and DreamerV3 on sepsis task.

D.3 Comparison between Clinician and Policy Predicted Actions

We compare the action distributions of MedDreamer and clinicians across both sepsis treatment (Figure8) and ventilator settings (Figure9). As shown in the joint action heatmaps, clinicians predominantly favored minimal IV fluid and vasopressor use, indicating a conservative treatment strategy. In contrast, MedDreamer exhibit a broader distribution, particularly with increased use of moderate vasopressor levels, suggesting a tendency toward more proactive hemodynamic intervention. Additionally, in terms of ventilator settings, MedDreamer generally adopt lower FiO₂ and tidal volumes compared to clinicians, aligning with lung-protective and oxygen-conservative strategies. While both approaches favor low PEEP settings, MedDreamer shows a slightly higher usage of elevated PEEP.

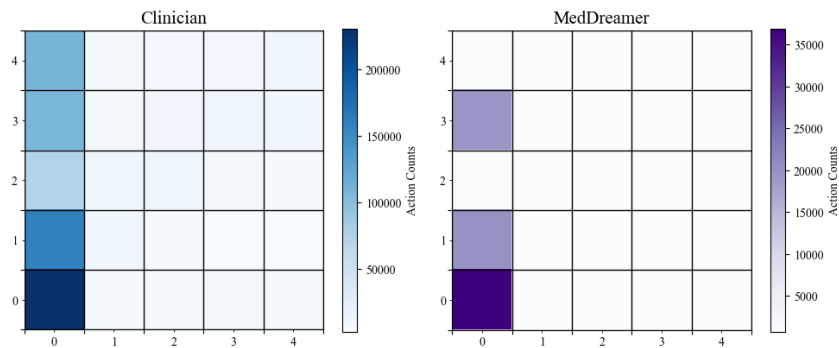


Figure 8: Differences between clinicians' actions and policy actions for sepsis task.

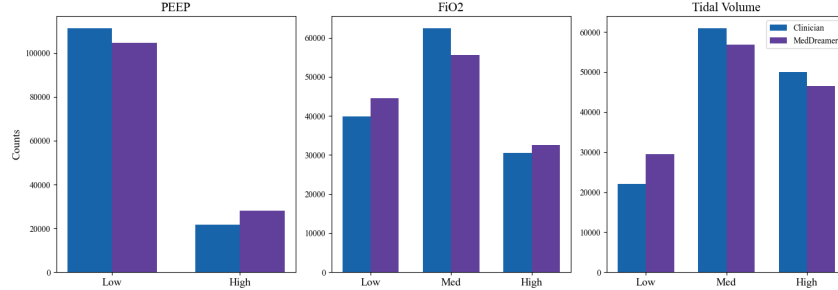


Figure 9: Differences between clinicians' actions and policy actions for MV task.

D.4 Stratification of Action Distribution

To assess how these learned policies align with clinician behavior, we further evaluate their performance against clinician-derived policies. We compare sepsis action distributions across SOFA severity levels to assess treatment adaptation among baseline models (see Figure 10). Clinicians displayed clear progression from conservative to aggressive interventions with increasing severity. MedDreamer closely follow this trend, especially in its increased use of vasopressors under high SOFA conditions. In contrast, model-free baselines like DDQN and EZ-Vent exhibit more diffuse and less interpretable action patterns, suggesting potential instability or lack of calibration. Other model-based methods such as MBRL-EHR and MBRL-BNN favor consistent low-level actions but lacked sufficient flexibility to adjust to patient severity. These results highlight MedDreamer's ability to learn severity-aware treatment strategies more aligned with clinical patterns.

D.5 Choice of Phase 1 for Policy Training

We conduct an ablation study to evaluate the impact of imagination and training strategies in both phases of MedDreamer on sepsis task. As shown in Table 7, we compared our default setting (MedDreamer with $\tau = 10$) against two alternatives that do not incorporate imagined trajectories in phase 1. P1-NoIm uses a conventional actor-critic approach with TD error computed on real transitions, while P1-RL adopts the replay loss from DreamerV3, where λ -returns are computed using real rewards sampled from a replay buffer. Both variants result in reduced effective sample size (ESS) and lower off-policy evaluation scores (V_CWPDIS), indicating that introducing even short imagined rollouts during phase 1 improves learning signals and downstream policy quality. We also test two additional variants for phase 2. First, we apply the phase 1 training pipeline (i.e., imagine additional steps in the time space per trajectory) to phase 2, and observe that the imagined episode return dropped significantly. We also test the MedDreamer phase 2 pipeline, the imagined episode return remain stuck at a low value throughout training. These results suggest that gradually increasing the role of imagination, which is starting with short imagined rollouts in phase 1 and progressing to full imagined trajectories in phase 2 is essential for stable training and effective policy learning.

Table 7: Results using other settings for phase 1 for sepsis task.

	ESS	V_CWPDIS	Imagined Episode Return
P1-RL	17.75	4.11	0.49
P1-NoIm	17.81	4.63	1.21
MedDreamer	22.88	4.75	5.64

D.6 Mortality vs. Return

We analyze the relationship between estimated return and predicted mortality across models for both the sepsis (Figure 11) and MV (Figure 12) tasks. Across both cohorts, MedDreamer consistently demonstrates the expected strong inverse correlation between return and mortality—higher estimated returns correspond to lower mortality, suggesting that the learned reward signal effectively captures clinically meaningful outcomes. In contrast, Dreamer exhibits an unexpected upward trend in mortality with increasing returns in the sepsis task, indicating misalignment between its learned

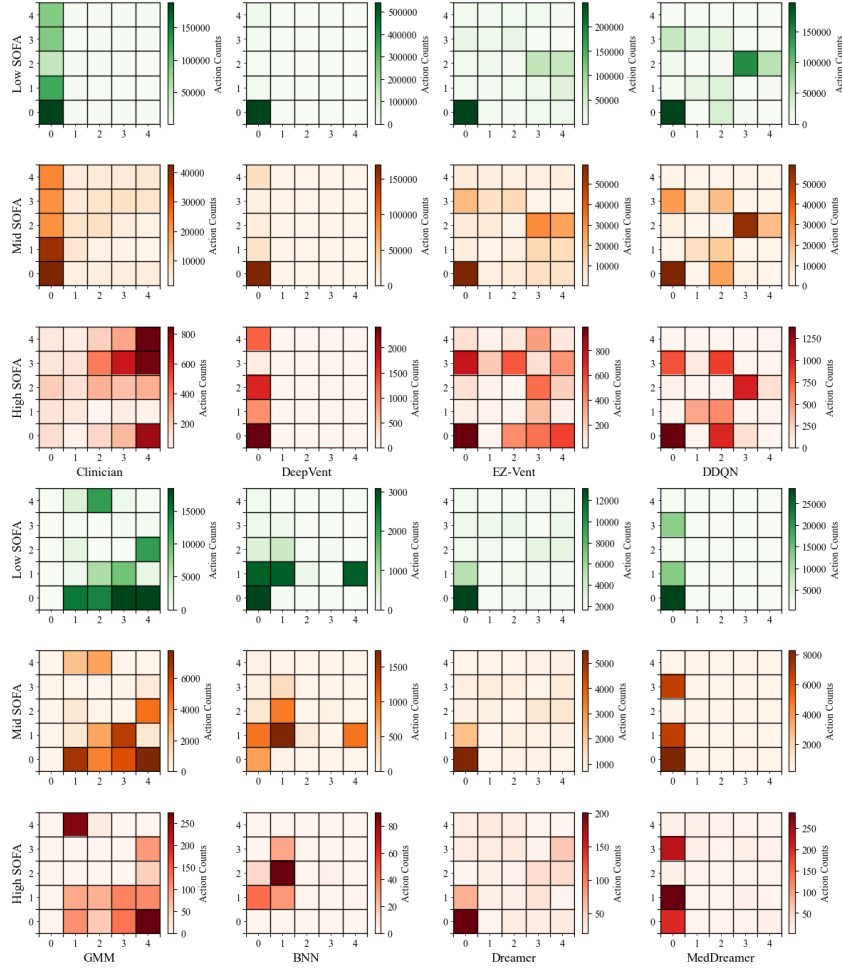


Figure 10: Treatment action distributions for sepsis task.

reward and actual patient outcomes. Model-free baselines such as DeepVent, EZ-Vent, and DDQN display generally flat or noisy trends, revealing limited correlation between return and mortality, and highlighting a lack of effective value shaping. Model-based EHR and BNN show moderate downward trends but with reduced magnitude and stability. Notably, clinician policies also show downward trends, validating the intermediate reward design. Overall, these findings reinforce MedDreamer’s ability to learn a return function that more faithfully reflects outcome-relevant clinical improvements, leading to more interpretable and trustworthy decision-making.

D.7 AI Episode Return

Figure13 compares the AI episode return and imagined episode return between MedDreamer-p1 and MedDreamer-p2 across training steps for sepsis task. The AI episode return, computed per transition on real patient data, reflects the policy’s effectiveness under the actual environment dynamics, while the imagined episode return summarizes cumulative reward over full trajectories generated by the latent dynamics model. In both metrics, MedDreamer-p2 consistently outperforms MedDreamer-p1. Specifically, MedDreamer-p2 achieves a higher and more stable AI episode return, indicating better generalization and clinical decision-making performance. It also exhibits a higher imagined episode return with lower variance, suggesting that its policy and world model are better aligned and more effective at generating useful imagined rollouts. The gap between MedDreamer-p1 and p2 further grows with training, highlighting the benefits of MedDreamer-p2’s enhanced fine-tuning strategy in leveraging imagination-based policy improvement. Together, these results confirm that MedDreamer-p2 achieves superior performance both in real and simulated environments.

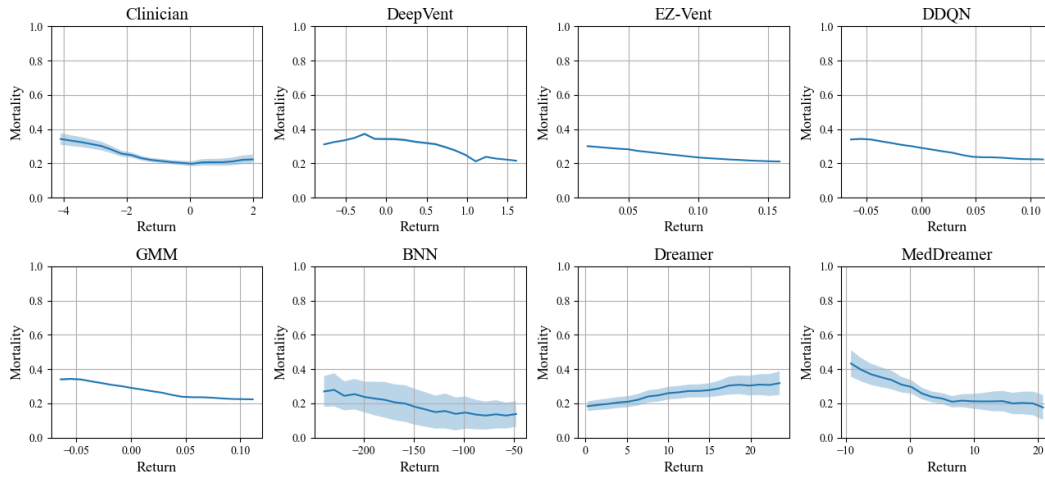


Figure 11: Mortality vs return plot including baselines for sepsis task.

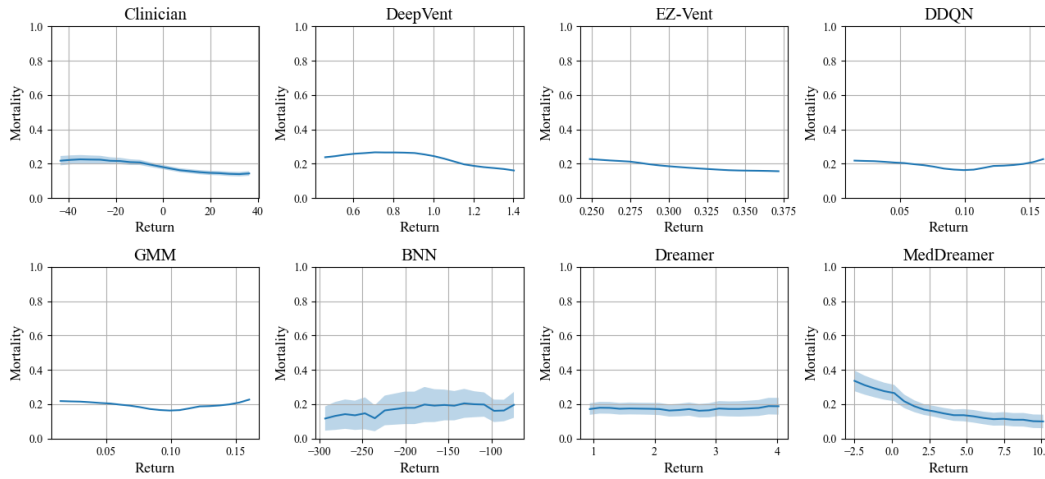


Figure 12: Mortality vs return plot including baselines for MV task.

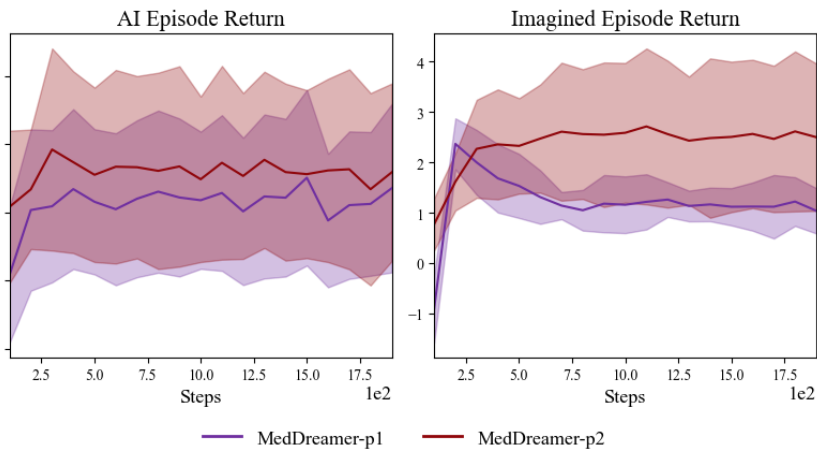


Figure 13: AI episode return and imagined episode return for sepsis task.

D.8 Choice of τ

We selected the value of τ , which controls the number of imagined steps during training, based on OPE metrics including ESS and V_CWPDIS. As shown in Figure 14, both metrics tend to decrease as the number of imagined steps increases, indicating that excessive imagination may introduce distributional mismatch. While $\tau = 5$ achieves the highest ESS, it yields lower V_CWPDIS compared to $\tau = 10$, suggesting weaker policy performance despite improved sample efficiency. We therefore chose $\tau = 10$ as the default, striking a balance between stable off-policy evaluation and effective policy improvement.

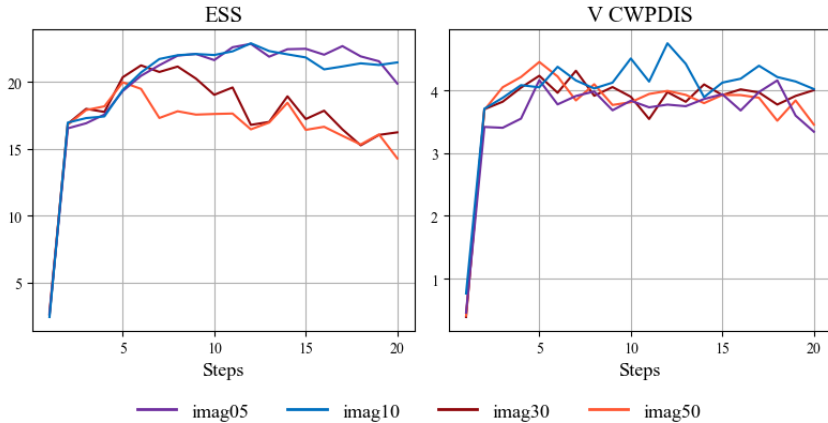


Figure 14: OPE metrics for different τ values.

E Broader Impact

We believe that MedDreamer is an important step toward applying reinforcement learning to personalized clinical decision-making, particularly for high-risk tasks such as sepsis treatment and mechanical ventilation management. By enabling policy learning in a structured latent space while relying on retrospective EHR data, our framework offers the potential to enhance treatment consistency, improve patient outcomes, and assist clinicians with reliable, data-driven support, in an ethical and clinically grounded training approach.

The framework is designed to complement, not compete the clinicians. MedDreamer’s capability to effectively integrate both real and simulated patient trajectories offers an opportunity to uncover previously unexplored or under explored, yet clinically driven scenarios, such as patterns that are difficult for human clinicians to detect, particularly in complex or rapidly evolving scenarios. As supported by the experimental results, we believe this could lead to improved patient outcomes, especially in resource-constrained environments or where standardization is lacking, such as in complex critical care. Additionally, these data driven systems could serve as a foundation for broader research into decision support systems that combine clinical reliability with generalizability, offering guidance for future systems that adapt across diverse patient population and care settings. The learned policies could even help explore previously under explored treatment processes, helping advance the clinical care research.

However, more comprehensive experimentation, scrutinized evaluations, and thoughtful deployment is needed. Similar with any AI-driven system, especial considerations are needed to ensure that the learned policies align with clinical standards, transparency of recommendations, and safeguards against biases in historical data. We believe MedDreamer as a step towards safe, collaborative, and intelligent clinical support, which would enable more equitable and effective healthcare when responsibly deployed.

F Limitations

MedDreamr addresses key healthcare treatment recommendation challenges and presents several innovations to learn effective treatment policies as evident from the conducted evaluations. However, **similar to the clinical decision support systems in literature**, it operates under some assumptions and constrains as follows:

- All models, including the baselines, are trained and evaluated on retrospective, observational data. Therefore the results rely on the fidelity of the learned reward function, and are limited by the absence of counterfactual ground truth.
- Performance of all the learned policies are assessed using estimated returns from a learned reward model. This provides an even ground for evaluation across all the tested models. Although we have followed the standard practice, this proxy measure may not perfectly capture true clinical utility.
- All experiments are conducted on MIMIC-IV and eICU datasets. MedDreamer was able to generalize better across the tested tasks, and shown superior generalizability among the models tested. However the generalizability beyond the tested tasks, hospitals or patient populations needs to be established before real-world deployments.
- While MedDreamer demonstrates improved estimated mortality, and close alignment to clinician policies in the past, additional assessments on clinician trustworthiness of the policy is needed with expert collaboration before real-world deployment.

Importantly, many of these limitations are not unique to MedDreamer, rather showcase broader challenges in deploying reinforcement learning systems in healthcare. Despite these, MedDreamer demonstrates strong performance, generalization, and clinical grounding. We see it as a principled and extensible foundation for future clinical decision support systems that prioritize reliability, and real-world applicability.